

Citation for published version:
Topolov, VY, Bowen, CR, Bisegna, P & Krivoruchko, AV 2015, 'New orientation effect in piezo-active 1-3-type composites', *Materials Chemistry and Physics*, vol. 151, pp. 187-195. https://doi.org/10.1016/j.matchemphys.2014.11.053

10.1016/j.matchemphys.2014.11.053

Publication date: 2015

Document Version Early version, also known as pre-print

Link to publication

University of Bath

Alternative formats

If you require this document in an alternative format, please contact: openaccess@bath.ac.uk

Copyright and moral rights for the publications made accessible in the public portal are retained by the authors and/or other copyright owners and it is a condition of accessing publications that users recognise and abide by the legal requirements associated with these rights.

Take down policyIf you believe that this document breaches copyright please contact us providing details, and we will remove access to the work immediately and investigate your claim.

Download date: 09. Mar. 2023

New orientation effect in piezo-active 1–3-type composites

V.Yu. Topolov^{a,*}, C.R. Bowen^b, P. Bisegna^c, A.V. Krivoruchko^d

^aDepartment of Physics, Southern Federal University, 5 Zorge Street, 344090 Rostov-on-Don, Russia

^bDepartment of Mechanical Engineering, University of Bath, Bath BA2 7AY, UK

Department of Civil Engineering and Computer Science, University of Rome "Tor Vergata", 00133 Rome, Italy

^dDon State Technical University, Gagarin Place, 344000 Rostov-on-Don, Russia

A B S T R A C T This paper studies the influence of the mutual orientation of the poling axes of single-crystal and ceramic components on the hydrostatic piezoelectric performance and anisotropy of squared figures of merit and electromechanical coupling factors for 1–0–3 composites that comprise two ferroelectric components and a piezo-passive polymer one. We demonstrate that the elastic and piezoelectric anisotropy of the 0–3 ferroelectric ceramic / polymer matrix with prolate inclusions leads to large hydrostatic piezoelectric coefficients d_h^* and g_h^* and squared figure of merit $d_h^* g_h^*$ in a 1–0–3 0.67Pb(Mg_{1/3}Nb_{2/3})O₃–0.33PbTiO₃ single crystal / (Pb_{1-x}Ca_x)TiO₃ ceramic / araldie composite with x=0.20–0.25. In this composite values of max $g_h^* \sim 10^2$ mV·m/N and max($d_h^* g_h^*$) $\sim 10^{-11}$ Pa⁻¹ are achieved in specific volume-fraction and rotation-angle ranges due to a new orientation effect in the presence of the highly anisotropic 0–3 matrix.

Keywords: A. Composite materials; D. Ferroelectricity; Piezoelectricity; Elastic properties *Corresponding author. Tel.:+7 863 2975127; fax:+7 863 2975120, E-mail: vutopolov@sfedu.ru

1. Introduction

Piezo-active composites are often regarded as heterogeneous materials that consist of two components, and at least one of them is piezoelectric. This piezoelectric component that is often selected is a poled ferroelectric ceramic with a relatively high piezoelectric activity, dielectric permittivity and other characteristics which play the important role in the formation of the effective electromechanical properties in the composite [a-1, a-2, a-3]. The composites based on ferroelectrics are the important group of modern smart materials wherein the effective properties and their anisotropy can be varied across a wide range and are useful for piezoelectric sensor, actuator, hydrophone and other applications [a-1, a-4, a-5].

An important trend in the study of advanced piezo-active composites in the last decade is a modification of its structure by introducing a third component that can enhance the piezoelectric performance, hydrostatic piezoelectric response and related parameters [1]. Among the composites with a high piezoelectric activity and/or sensitivity [2], of particular interest are those based on domain-engineered relaxor-ferroelectric single crystals (SC) [3], e.g. (1– x)Pb(Mg_{1/3}Nb_{2/3})O₃ – xPbTiO₃ (PMN–xPT) or (1–x)Pb(Zn_{1/3}Nb_{2/3})O₃ – xPbTiO₃. Poling these SCs in different directions lead to a polarisation orientation effect [2] in two-component SC / polymer composites with 1–3, 2–2 and 0–3 connectivities. This orientation effect depends not only on the connectivity of the composite sample, but also on the electromechanical properties of its SC component. We add that the polarisation orientation effect was studied in ferroelectric ceramic / polymer composites with 2–2, 3–3, 1–3, and 0–3 [a-1, a-2, a-6, a-7, a-8, a-8prim] connectivities. An improvement of the hydrostatic piezoelectric response in a 1–3 composite is achieved in the presence of a system of ceramic rods that are obliquely embedded into a polymer matrix [a-8prim]. Moreover, an example where the perforance a 1–3 composite with ceramic rods with a preferred orientation was considered in work [a-8duo].

The presence of an anisotropic piezoelectric matrix in a composite sample opens up new possibilities to vary the effective electromechanical properties of this composite and its hydrostatic parameters. In this case an important challenge is to explore links between the

effective properties of the composite as a whole and the anisotropic properties of its components at variations of the polarisation directions, microgeometric characterisitics, sizes of inclusions, and poling degree of components. The research problem concerned with such linkages in piezo-active composites is difficult and has not been discussed in detail. We note that an influence of the polarisation orientation in the heterogeneous (composite) matrix on the effective properties is yet to be analysed for three-component composites based on relaxor-ferroelectric SCs, i.e., for composites with the SC component that exhibits the strong piezoelectric effect in comparison to the two-component matrix. In this context, three-component composites that consist of two ferroelectric components (both SC and ceramic) and a polymer have yet to be studied in detail.

In this paper we first demonstrate that the different polarisation directions of the ferroelectric components with distinct differences in their electromechanical properties lead to an important 'orientation effect' and improved effective parameters for the three-component composite system. Undoubtedly, novel piezo-active three-component composites with two ferroelectric components may be of interest due to the complex inter-relationships in the fundamental triangle of 'composition – structure – properties'. The aim of the present paper is to analyse this orientation effect and some aforementioned relations in the context of the piezoelectric response of the three-component (SC/ceramic/polymer) composite system.

2. Model concepts and effective parameters

2.1. Model of the three-component composite

The composite studied in this paper consists of long SC rods embedded in a heterogeneous matrix (Fig.1,a). The SC rods are in the form of the rectangular parallelepiped with a square base and square arrangement in the (X_1OX_2) plane. The main crystallographic axes of each SC rod with the spontaneous polarisation $P_s^{(1)}$ are oriented as follows: $X||OX_1, Y||OX_2$ and $Z||P_s^{(1)}||OX_3$. The ferroelectric ceramic is used as an inclusion in the polymer matrix. The shape of each ceramic inclusion is spheroidal and obeys the equation $(x_1'/a_1)^2 + (x_2'/a_2)^2 + (x_3'/a_3)^2 = 1$ relative to the axes of the rectangular co-ordinate system $(X_1'X_2'X_3')$ rotated by an angle α with respect to

 $(X_1X_2X_3)$ (inset 1 in Fig.1,a). The semi-axes of each ceramic inclusion are $a_1=a_2$ and a_3 , the aspect ratio is $\rho_i=a_1/a_3$, and centres of the inclusions (Fig.1,b) occupy sites of a simple tetragonal lattice with unit-cell vectors parallel to the OX_k' axes. We assume that $0 < \rho_i < 1$, and the presence of prolate inclusions facilitates a poling of the ferroelectric ceramic / polymer matrix due to a weaker depolarisation effect therein. A remanent polarisation vector of each ceramic inclusion is $P_i^{(2)} \uparrow OX_3'$, and OX_3' is the poling axis of the matrix (inset 2 in Fig.1,a) that represents a composite with 0–3 connectivity in terms of work [1,2]. The three-component composite (Fig.1,a) is described by 1–0–3 connectivity. We add that methods to form a 0–3 matrix consisting of ceramic inclusions in a polymer for the 0–3 PbTiO₃-type ceramic / epoxy resin system include electric-field structuring [4], and other methods [3, a-1, a-2, a-5] have been used to form the 1–3 composite architecture which include a rod placement, dice and fill, etc. Assuming that the linear sizes of the inclusions in the 0–3 matrix are much smaller than the length of the side of the square being intersected the rod in the (X_1OX_2) plane, we evaluate the effective properties of the complete 1–0–3 composite in two stages.

2.2. First stage of averaging

Taking into account the electromechanical interaction between the piezo-active (poled ferroelectric ceramic) inclusions, the effective properties of the 0–3 composite are determined by means of the effective field method (EFM) [1,2]. Based on the EFM concepts [1, 2], we describe an electromechanical interaction in the system of 'ferroelectric ceramic inclusions – polymer matrix' (see inset 2 in Fig.1,a) using a local electric field that acts on each rod. This effective field is determined by taking into account a system of interacting inclusions and boundary conditions concerned with the spheroidal shape of each inclusion. The boundary conditions involve components of electric and mechanical fields at the inclusion – matrix interface. Following the EFM, we characterise the effective properties of the 0–3 composite by the 9×9 matrix [2]

$$|| C_{0-3} * || = || C^{(2)} || + m_i (|| C^{(1)} || - || C^{(2)} ||) [|| I || + (1 - m_i) || S || || C^{(2)} ||^{-1} (|| C^{(1)} || - || C^{(2)} ||)]^{-1}.$$

Matrices of electromechanical constants of components $||C^{(n)}||$ from Eq. (1) are

represented as follows:
$$\|C^{(1)}\| = \begin{pmatrix} ||c^{(1),E}|| & ||e^{(1)}||^t \\ ||e^{(1)}|| & -||\varepsilon^{(1),\varepsilon}|| \end{pmatrix}$$
 (ferroelectric ceramic) and

$$||C^{(2)}|| = \begin{pmatrix} ||c^{(2),E}|| & ||e^{(2)}||^t \\ ||e^{(2)}|| & -||\varepsilon^{(2),E}|| \end{pmatrix}$$
(polymer). In Eq. (1) m_i is the volume fraction of the ceramic

component, ||I|| is the identity matrix, and ||S|| is the matrix that contains the Eshelby tensor components [a-9] depending on the elements of $||C^{(2)}||$ and the aspect ratio ρ_i . In $||C^{(n)}||$ from Eq. (1), $||c^{(n),E}||$, $||e^{(n)}||$ and $||e^{(n),\xi}||$ comprise of the elastic moduli (at electric field E= const), piezoelectric coefficients and dielectric permittivities (at mechanical strain ξ = const), respectively, and the superscript t denotes the transposition. The effective electromechanical properties of the 0–3 ceramic / polymer composite are represented according to Eq. (1) in the

matrix form as
$$\|C_{0-3}^*\| = \begin{pmatrix} ||c_{0-3}^{*E}|| & ||e_{0-3}^*||' \\ ||e_{0-3}^*|| & -||\varepsilon_{0-3}^{*\varepsilon}|| \end{pmatrix}$$
, where $\|c_{0-3}^{*E}\|$, $\|e_{0-3}^*\|$ and $\|\varepsilon_{0-3}^{*\xi}\|$ depend on m_i

and ρ_i .

An alternative way to determine the effective properties of the heterogeneous matrix is the use of the finite element method (FEM) [2] and different meshes of the 0–3 structure, and in this paper we examine and compare both approaches. The COMSOL package [a-10] is applied to obtain the volume-fraction dependence of the effective electromechanical properties of the 0–3 composite within the framework of the FEM. A representative unit cell, containing the spheroidal inclusion with a radius adjusted to yield the appropriate volume fraction m_i , is discretised using tetrahedral elements [2]. Their number, depending on the aspect ratio ρ_i of the spheroidal inclusion, varies from 320,000 to 1,120,000. [Paolo, please check – maybe these values are not very correct...1 The unknown displacement and electric-potential fields are interpolated using linear Lagrangian shape functions. The corresponding number of degrees of freedom varies from 200,000 to 800,000*). [Paolo, please check – maybe these values are not very correct...1

For what concerns the conditions at the inclusion – matrix interface in FEM computations, the following conditions have been assumed: (i) perfect bonding (i.e., continuity of the displacement field) and (ii) continuity of the electric potential. Moreover, the periodic boundary conditions were assumed on the boundary of the parallelepipedic representative unit cell 'inclusion – matrix'. The matrix of effective electromechanical constants of the 0–3 composite is computed column-wise, performing calculations for diverse average strain and electric fields imposed to the structure. The Geometric Multigrid [a-11] iterative solver (V-cycle, successive over-relaxation pre- and post-smoother, direct coarse solver) is employed. After solving the electroelastic equilibrium problem, the effective electromechanical constants of the 0–3-composite are computed, by averaging the resulting local stress and electric-displacement fields over the representative unit cell. As in the EFM, the matrix of the effective electromechanical properties $\|C_{0-3}^*\|$ determined using the FEM is a function of m_i and ρ_i .

Using either the EFM or FEM and taking into account the rotation $(X_1'X_2'X_3') \rightarrow (X_1X_2X_3)$, we find the matrix of effective electromechanical properties $||C_{0-3}^*|| = ||C_{0-3}^*(m_i, \rho_i, \alpha)||$ in the co-ordinate system $(X_1X_2X_3)$. As is seen from inset 1 in Fig.1,a, the rotation is carried out around the (OX_1) axis, and the matrix is given by $||r|| = \begin{pmatrix} 1 & 0 & 0 \\ 0 & \cos\alpha & \sin\alpha \\ 0 & -\sin\alpha & \cos\alpha \end{pmatrix}$.

2.3. Second stage of averaging

The effective properties of the 1–3-type composite with planar interfaces (i.e., the system of the long SC parallelepiped-shaped rods in the 0–3 matrix) are evaluated using the matrix method [2]. Hereby we average the electromechanical properties of the SC rod and 0–3 composite matrix in the OX_1 and OX_2 directions, in which the periodic structure of the composite

^{*)} For instance, the mesh (Fig.1,c) used for FEM computations of the effective properties of the 0–3 composite at $\rho_i = 0.3$ and $m_i = 0.1$ comprises 1,118,006 tetrahedral elements, and the number of degrees of freedom solved for these computations is 775,604.

(Fig.1,a) is observed, and take into account electromechanical interactions in a system of 'piezo-active rods – piezo-active matrix'.

The matrix of the effective properties $\parallel C^* \parallel$ is determined by averaging the electromechanical properties of the components (SC and 0-3 composite) on the volume fraction m and is given by

$$||C^*|| = [||C_{SC}|| \cdot ||M||m + ||C_{0-3}^*||(1-m)] \cdot [||M||m + ||I||(1-m)]^{-1},$$
(2)

where $\|C_{SC}\|$ and $\|C_{0-3}^*\|$ are matrices of the electromechanical properties of the SC and 0–3 composite, respectively, $\|M\|$ is used to take into account the electric and mechanical boundary conditions [2] at interfaces $x_1 = \text{const}$ and $x_2 = \text{const}$ (Fig. 1,a), and $\|I\|$ is the identity matrix. For example, the boundary conditions at $x_1 = \text{const}$ imply a continuity of components of mechanical stress $\sigma_{11} = \sigma_1$, $\sigma_{12} = \sigma_6$ and $\sigma_{13} = \sigma_5$, strain $\xi_{22} = \xi_2$, $\xi_{23} = \xi_4/2$ and $\xi_{33} = \xi_3$, electric displacement D_1 , and electric field E_2 and E_3 . We add that $\|C_{SC}\|$ and $\|C_{0-3}^*\|$ are written as $\|C_{SC}\| = \|C_{SC}\| \|$

$$\|C_{SC}\| = \begin{pmatrix} \|s_{SC}^E\| & \|d_{SC}\|^t \\ \|d_{SC}\| & \|\varepsilon_{SC}^\sigma\| \end{pmatrix} \text{ and } \|C_{0-3}^*\| = \begin{pmatrix} \|s^{*E}\| & \|d^*\|^t \\ \|d^*\| & \|\varepsilon^{*\sigma}\| \end{pmatrix}, \text{ where } s^E, d \text{ and } \varepsilon^\sigma \text{ are elastic}$$
compliance at $E = \text{const}$, piezoelectric coefficient and dielectric permittivity at $\sigma = \text{const}$,

respectively. A transition from $\|c_{0-3}^{*E}\|$, $\|e_{0-3}^*\|$ and $\|\varepsilon_{0-3}^{*g}\|$ (the matrices determined for the 0–3 composite in Section 2.2) to $\|s_{0-3}^{*E}\|$, $\|d_{0-3}^*\|$ and $\|\varepsilon_{0-3}^{*o}\|$ is carried out taking into consideration conventional formulae [a-12] for a piezoelectric medium. Thus, based on Eq. (2), we finally represent the effective properties of the 1–0–3 composite in the co-ordinate system $(X_1X_2X_3)$ as

$$|| C^* || = || C^*(m, m_i, \rho_i, \alpha) || = \begin{pmatrix} || s^{*E} || & || d^* ||^t \\ || d^* || & || \varepsilon^{*\sigma} || \end{pmatrix}.$$
(3)

2.4. Components and effective parameters

Among the potential active components of interest, we choose a [001]-poled domain-engineered PMN-0.33PT SC (main component in a 1–3 composite [3]), poled (Pb_{1-x}Ca_x)TiO₃ ceramic and piezo-passive araldite polymer (Table 1). The PMN-0.33PT SC with a composition near the morphotropic phase boundary is chosen since it exhibits a very high piezoelectric

activity and moderate piezoelectric anisotropy [5], while the $(Pb_{1-x}Ca_x)TiO_3$ ceramic with $0.20 \le x \le 0.25$ has been selected for its contrasting properties, since it exhibits only a moderate piezoelectric activity, but has a large piezoelectric anisotropy [6]. As is known from experimental data [5,8], the coercive fields $E_c^{(n)}$ of the PMN–xPT SC (n=1) and $(Pb_{1-x}Ca_x)TiO_3$ ceramic (n=2) satisfy the condition $E_c^{(1)} << E_c^{(2)}$. This condition enables initial poling of the 0–3 matrix under a strong electric field with a subsequent poling of the SC rods in the composite (Fig.1,a) under a less intensive electric field. It should be added that $(Pb_{1-x}Ca_x)TiO_3$ and related highly anisotropic ceramics were used to form 0–3 ceramic / polymer composites, and some parameters of these composites are given in Refs.a-13, a-14.

Based on the full set of electromechanical constants from Eqs. (2) and (3), we determine the following effective parameters of the 1–0–3 composite: piezoelectric coefficients g_{fl}^* from equation $||d^*|| = ||\varepsilon^{*\sigma}|| \cdot ||g^*||$, squared strain–voltage figures of merit

$$(Q_{33}^*)^2 = d_{33}^* g_{33}^*, (Q_{32}^*)^2 = d_{32}^* g_{32}^* \text{ and } (Q_{31}^*)^2 = d_{31}^* g_{31}^*,$$
 (4)

electromechanical coupling factors

$$k_{33}^* = d_{33}^* / (\varepsilon_{33}^{*\sigma} s_{33}^{*E})^{-1/2}, k_{32}^* = d_{32}^* / (\varepsilon_{33}^{*\sigma} s_{22}^{*E})^{-1/2}$$
 and $k_{31}^* = d_{31}^* / (\varepsilon_{33}^{*\sigma} s_{11}^{*E})^{-1/2},$ (5)

hydrostatic piezoelectric coefficients

$$d_b^* = d_{33}^* + d_{32}^* + d_{31}^* \text{ and } g_b^* = g_{33}^* + g_{32}^* + g_{31}^*,$$
 (6)

and squared hydrostatic figure of merit

$$(Q_h^*)^2 = d_h^* g_h^*. (7)$$

It is assumed that electrodes applied to a composite sample are perpendicular to the OX_3 axis. Squared figures of merit $(Q_{fl}^*)^2$ from Eqs.(4) are an indicator of the sensor signal-to-noise ratio of the composite and its piezoelectric sensitivity. Electromechanical coupling factors k_{fl}^* from Eqs.(5) describe the effectiveness of the energy conversion from the mechanical form into the electric one and vice versa along the co-ordinate axes and is of interest for energy harvesting applications. Hydrostatic piezoelectric coefficients d_h^* and g_h^* from Eqs.(6) describe the piezoelectric activity and sensitivity under hydrostatic loading of the composite sample for SONAR and hydrophone applications. The parameter $(Q_h^*)^2$ from Eq.(7) serves as a hydrostatic analog of $(Q_{3l}^*)^2$ from Eqs.(4) and is used [1,2] to characterise the piezoelectric sensitivity under hydrostatic loading. Due to the variable anisotropy of piezoelectric coefficients in the 0–3 matrix at changing the rotation angle α , we distinguish the piezoelectric response of the 1–0–3 composite along the OX_1 and OX_2 axes. As a consequence, in a general case, expressions $(Q_{31}^*)^2 \neq (Q_{32}^*)^2$, $k_{32}^* \neq k_{31}^*$, $d_{32}^* \neq d_{31}^*$, and $g_{32}^* \neq g_{31}^*$ hold. We remind the reader that for a conventional 1–3 ceramic / polymer composite poled along the OX_3 axis, relations $(Q_{31}^*)^2 = (Q_{32}^*)^2$, $k_{32}^* = k_{31}^*$, $d_{32}^* = d_{31}^*$, and $g_{32}^* = g_{31}^*$ are valid [a-3, a-4, 2] because of the transverse isotropy.

3. Results and discussion

The piezoelectric properties of the 1–3–0 composite (Fig. 1,a) at $\alpha \neq 0^{\circ}$, $\alpha \neq 180^{\circ}$ and $0 < m < 180^{\circ}$

1 are represented by a matrix
$$||p^*|| = \begin{pmatrix} 0 & 0 & 0 & 0 & p_{15}^* & p_{16}^* \\ p_{21}^* & p_{22}^* & p_{23}^* & p_{24}^* & 0 & 0 \\ p_{31}^* & p_{32}^* & p_{33}^* & p_{34}^* & 0 & 0 \end{pmatrix}$$
, where $p = d$, e , g , or h . This

composite belongs to the m symmetry class at the mirror plane perpendicular to OX_1 . Taking into account the rotation mode and symmetry of the components, we find that the effective properties and parameters from Eqs.(2)–(5) obey the condition $\Pi^*(m, m_i, \rho_i, \alpha) = \Pi^*(m, m_i, \rho_i, 360^\circ - \alpha)$. Hereafter we consider examples of orientation (α) and volume-fraction (m or m_i) dependences of the effective parameters of the 1–3–0 composite at ρ_i = const in its 0–3 matrix.

3.1. Volume-fraction dependence of the hydrostatic piezoelectric coefficient $\,g_{\scriptscriptstyle h}^{^*}\,$ at various α

The graphs in Fig. 2 show that local max g_h^* is observed at relatively small volume fractions of the SC component $(0.01 \le m \le 0.05)$. The $g_h^*(m)$ dependence is typical of 1–3 composites irrespective of the main piezoelectric component [a-4, 2]. This behaviour stems from rapid increase in $|d_{3j}^*|$ and relatively slow increase of ε_{33}^{*o} at m << 1 in the 1–3 composite where

the system of aligned piezoelectric rods plays a key role in his behaviour. Comparing graphs in Fig. 2, a, b and c, it can be seen that the local max g_h^* is related to $\alpha \approx 90^\circ$, and the value of max g_h^* considerably depends on the volume fraction of the ceramic inclusions m_i in the 0–3 matrix. This means that changes in m_i influence the dielectric permittivity $\varepsilon_{33,0-3}^{*o}$ of the 0–3 matrix and, therefore, ε_{33}^{*o} of the composite as a whole. Increasing ε_{33}^{*o} with increasing m_i leads to a decrease in both $|g_{3j}^*|$ and g_h^* , and this trend can be seen when comparing maximum points of g_h^* in Fig. 2,a–c.

We underline that when the volume fraction of the SC component is near m = 0.05, values of $g_h^* \approx (120-140) \,\text{mV·m}/\text{N}$ are achieved (Fig. 2, a–c), and at m > 0.05 the orientation effect becomes less pronounced at various volume fractions m_i , even in the presence of the highly prolate ceramic inclusions ($\rho_i << 1$) in the 0–3 matrix. This behaviour a result of the important role of the dielectric properties of the 0–3 matrix: it is seen that the influence of $\varepsilon_{33,0-3}^{*o}$ on ε_{33}^{*o} and g_h^* of the composite remains strong with changes in both m_i and α . An additional reason of this behaviour may be associated with changes in an elastic anisotropy of the 0–3 matrix at changes in m_i and α .

Comparing Fig. 2,b and 2,d, we state that a transition from a highly prolate inclusion (at ρ_i = 0.1) to a less prolate inclusion (at ρ_i = 0.3) in the 0–3 matrix leads to a distinct decrease in g_h^* near its local maximum at 80° $\leq \alpha \leq$ 100°, see curves 2–4 in Fig. 2,b,d. This means that with increasing ρ_i , a significant orientation effect is detected in a more narrow α range, and this feature is accounted for by the less pronounced anisotropy of the piezoelectric properties in the 0–3 matrix at larger values of ρ_i .

3.2. Orientation dependence of the hydrostatic piezoelectric response

The orientation dependence of the hydrostatic parameters (Fig.3,a,b) suggests that max g_h^* and max[$(Q_h^*)^2$] are achieved at a rotation angle $\alpha \approx 90^\circ$ with a volume fraction of ceramic

inclusions m_i = 0.12. Local max g_h^* may be found at the volume fraction of SC 0.01< m< 0.12, however the fabrication at the volume fractions m< 0.03 may be problematic in terms of the manufacturing tolerance [2]. The largest value of g_h^* at $0.1 \le \rho_i \le 0.5$ is related to $m_i \approx 0.12$ and 0.01< m< 0.03, and in this m range local max g_h^* is observed at various values of m_i , ρ_I and α (Fig. 2). Our evaluations based on the EFM (0–3 matrix) and matrix method (1–3-type composite) lead to absolute max d_h^* = 305 pC/N at m= 0.532, m_i = 0.12, ρ_i = 0.1, and α = 90°.

Using the matrix method, for the 1–3 PMN–0.33PT SC / araldite composite we find absolute max $g_h^* = 158$ mV·m/N, max[$(Q_h^*)^2$]= 8.27·10⁻¹² Pa⁻¹ and max $d_h^* = 274$ pC/N at m = 0.016, 0.103 and 0.509, respectively. At m = 0.05 for the 1–3 PMN–0.33PT SC / araldite composite we obtain $g_h^* = 115$ mV·m/N, and this value is considerably smaller than g_h^* near maxima in Figs.2 and 3,a.

The large values of $(Q_h^*)^2$ (Fig.3,b) and d_h^* in the 1–0–3 composite are due to the presence of the 0–3 matrix based on the ceramic with the piezoelectric coefficients $d_{3f}^{(2)}$ that obey the condition [6] $d_{33}^{(2)}/|d_{31}^{(2)}| >> 1$. At $\alpha = 90^\circ$, the remanent polarisation vector $P_r^{(2)}$ of each ceramic inclusion (inset 2 in Fig.1,a) is parallel to OX_2 , and this $P_r^{(2)}$ orientation leads to a decrease in $|d_{32}^*|$ with minor changes in d_{31}^* and d_{33}^* (or g_{31}^* and g_{33}^* , respectively) as a result of the weak lateral piezoelectric effect in the 0–3 matrix. As a consequence of the reduced $|d_{32}^*|$, we observe an increase in both d_h^* and g_h^* .

The elastic anisotropy of the 0–3 matrix with highly prolate inclusions is an additional factor in increasing the hydrostatic parameters (6) and (7). For example, ratios of the elastic compliances of the 0–3 (Pb_{0.75}Ca_{0.25})TiO₃ ceramic / araldite composite are $s_{11,0-3}^E/s_{12,0-3}^E=-2.21$, $s_{11,0-3}^E/s_{13,0-3}^E=-6.52$ and $s_{11,0-3}^E/s_{33,0-3}^E=1.95$ at $\rho_i=0.1$ and $m_i=0.10$. At $\rho_i=0.3$ and $m_i=0.10$ in the same composite there are $s_{11,0-3}^E/s_{12,0-3}^E=-2.52$, $s_{11,0-3}^E/s_{13,0-3}^E=-3.51$ and $s_{11,0-3}^E/s_{33,0-3}^E=1.25$, i.e., a significant decrease of $|s_{11,0-3}^E/s_{13,0-3}^E|$ and $|s_{11,0-3}^E/s_{33,0-3}^E|$ is observed with a weakening of the

piezoelectric activity. This *orientation effect* in the 1–0–3 composite favours an increase in $(Q_h^*)^2$ and d_h^* near its maxima by approximately 29% and 11%, respectively, in comparison to a 'traditional' two-component 1–3 PMN–0.33PT SC / araldite composite. The studied 1–0–3 composite is also attractive due to large values of local maxima of d_h^* , g_h^* and $(Q_h^*)^2$ at m_i = const, especially at $m_i < 0.15$.

3.3. Anisotropy of figures of merit and electromechanical coupling factors

The inequality

$$(Q_{33}^*)^2/(Q_{3i}^*)^2 \ge 10 \ (j=1 \text{ and } 2)$$
 (8)

holds at volume fractions of SC $m_{Q1} \le m \le m_{Q2}$ which depend on the rotation angle α (Fig.3,c). The validity of condition (8) is due to the presence of the 0–3 matrix which has a significant elastic and piezoelectric anisotropy at $m_i = 0.50$ and $\rho_i = 0.1$. In this case the prolate ceramic inclusions have a significant influence on the electromechanical properties of the 0–3 matrix, and the anisotropy of these properties is very favourable to detect the orientation effect in the 1–0–3 composite. Values of $m_{Q2} < 0.1$ may be a result of the high piezoelectric activity of the SC while $d_{33}^{(1)}/d_{33}^{(2)} \approx 100$. We note that $(Q_{33}^{(1)})^2/(Q_{31}^{(1)})^2=(Q_{33}^{(1)})^2/(Q_{32}^{(1)})^2=(d_{33}^{(1)}/d_{31}^{(1)})^2\approx 4.5$ is related to the PMN–0.33PT SC (see Table 1).

The electromechanical properties of the 0-3 matrix favour the inequality

$$|k_{33}^*/|k_{3i}^*| \ge 5$$
 (9)

that is valid at $m_{k1} \le m \le m_{k2}$ (Fig. 3, d). Taking into account Eqs. (5), we state that the ratio (9) depends strongly on the piezoelectric and elastic anisotropy of the SC and ceramic, and this anisotropy remains distinct at relatively small values of m. Our evaluations at fixed values of m_{k2} and α from Fig.3,d show that the longitudinal electromechanical coupling factor k_{33}^* monotonically decreases from 0.507 (α = 0°) to 0.292 (α = 21°). Based on data from Table 1, we highlight for comparison that $k_{33}^{(2)} = 0.290$ for the (Pb_{0.75}Ca_{0.25})TiO₃ ceramic.

3.4. g_{3j}^* versus d_{3j}^*

Examples of a dependence of the piezoelectric coefficients d_{3j}^* and g_{3j}^* on the rotation angle α at relatively small SC volume fractions m are shown in Fig.3,e,f. A comparison of the graphs in Fig.3,e and f suggests that the orientation effect is inseparably linked with the lateral piezoelectric response of the 1–0–3 composite. This means that the effect of the anisotropic 0–3 matrix on d_{3j}^* and g_{3j}^* is more pronounced near α = 90°, i.e. in a case when the piezoelectric anisotropy of the ceramic inclusions promotes a large contribution from the piezoelectric coefficient of the 0–3 matrix $d_{32,0-3}^* > 0$ into $d_{32}^* < 0$ of the 1–0–3 composite. As a result, we see a large difference between d_{31}^* and d_{32}^* (cf. curves 7–9 and 10–12 in Fig.3,e), and $|d_{31}^*| > |d_{32}^*|$ because of lack of the aforementioned contribution into $d_{31}^* < 0$ due to the rotation axis OX_1 (see inset 1 in Fig.1,a).

Increasing the aspect ratio ρ_i of the ceramic inclusion in the polymer medium leads to a weaker piezoelectric effect in the 0–3 matrix, lower values of $|s_{11,0-3}^E/s_{13,0-3}^E|$ and $|s_{11,0-3}^E/s_{33,0-3}^E|$, and a decrease of the hydrostatic parameters (6) and (7). For example, the 1–0–3 PMN–0.33PT SC / (Pb_{0.75}Ca_{0.25})TiO₃ ceramic / araldite composite at ρ_i = 0.3 is characterised by local max d_h^* = 279 pC/N and 278 pC/N at m_i = 0.10 and 0.15, respectively, as well as by local max[$(Q_h^*)^2$]= 8.47·10⁻¹² Pa⁻¹ and 7.98·10⁻¹² Pa⁻¹ at m_i = 0.10 and 0.15, respectively. This means that the anisotropy of the piezoelectric coefficients d_{3j}^* remains important with changes in the microgeometry of the 0–3 matrix and influences behaviour of g_{3j}^* , d_h^* , g_h^* and $(Q_h^*)^2$. Replacing the (Pb_{0.75}Ca_{0.25})TiO₃ ceramic with (Pb_{1-x}Ca_x)TiO₃ at x= 0.20–0.24 leads to changes in the parameters (4)–(7) of the 1–0–3 composite by 1–3%. As is known from Ref. 6, the (Pb_{1-x}Ca_x)TiO₃ ceramics at x= 0.20–0.24 are characterised by piezoelectric coefficients d_{3j} that obey conditions for the large piezoelectric anisotropy: e.g., $d_{33}^{(2)}/|d_{31}^{(2)}|$ = 18.7, 30.3 and 39.8 at x= 0.20, 0.23 and 0.24, respectively.

lead titanate compositions [8]. In our opinion, the large piezoelectric anisotropy of the $(Pb_{1-}xCa_x)TiO_3$ ceramics leads to the large piezoelectric anisotropy of the 0–3 composite and favours a stable behaviour of effective parameters from Eqs. (4)–(7) and the orientation effect in the 1–0–3 composite.

3.5. Comparison of effective parameters of composites

The effective parameters obtained using different methods applied to the 0–3 matrix (see Section 2.2) are compared in Table 2. In addition to the EFM approach, two FEM models are considered. Either Dirichlet (FEM-1) or periodic (FEM-2) boundary conditions are enforced on the boundary of the representative unit cell, and the matrix of effective constants of the 0–3 ceramic-polymer matrix (inset 2 in Fig.1,a) is computed column-wise, performing calculations for diverse average strain and electric fields imposed to the structure. The use of Dirichlet boundary conditions gives rise to a higher piezoelectric activity of the 0–3 matrix, whereas periodic boundary conditions lead to a lower piezoelectric activity than that obtained using the EFM method. The EFM results are close to average values obtained from the FEM models. Relatively small differences between the parameters obtained using the EFM, FEM-1 and FEM-2 (Table 2) are due to the very high piezoelectric activity of the SC rod in comparison to the 0–3 matrix surrounding it.

Since this is the first study of the performance of the novel 1–0–3 composite (Fig. 1,a) and the orientation effect therein, it is impossible to compare the predicted effective parameters (Figs.2 and 3 and Table 2) directly to those known from literature experimental data for this composite. Nevertheless, we now compare some effective parameters of this novel composite to those related to some well known two-component composites. For example, a 1–3 PMN–0.30PT SC / epoxy composite is characterised by experimentally determined values of the piezoelectric coefficient $g_{33}^* \approx (90-130)$ mV.m/N at volume fractions of the SC component m = 0.26-0.70 [a-5]. A predicted value of max $g_{33}^* \approx 400$ mV.m/N (at m < 0.05) [a-5] is comparable to values typical of the 1–0–3 composite at m = 0.05 and $m_i = 0.10-0.15$ (Fig.3,f). In a 1–3 PZT ceramic /

epoxy composite with a preferred orientation of ceramic rods [a-8duo], values of max $d_h^* \approx 110$ pC / N and max[$(Q_h^*)^2$]= 6.0·10⁻¹² Pa⁻¹ are considerably less than the maximum values of these parameters of the 1–0–3 composite (see, for instance, Fig.3, b and Table 2). In a (Pb_{0.75}Ca_{0.25})TiO₃ ceramic / copolymer vinylidene fluoride-trifluorethylene composite with elements of 0-3 and 1-3 connectivity patterns, the piezoelectric coefficient g_{33}^* decreases from 161 to 106 mV m/N with increasing the volume fraction of ceramic from 0.20 to 0.60 [a-14]. The presence of two piezoelectric components, namely, ferroelectric ceramic and polymer, do not lead to a considerable increase of g_{33}^* in the composite [a-14] based on (Pb_{0.75}Ca_{0.25})TiO₃. According to data [a-15], a 1–3 PMN–0.33PT SC / araldite composite is characterised by max d_h^* = 274 pC/N (at m = 0.509), max $g_h^* = 130$ mV m/N (at m = 0.016) and max[$(Q_h^*)^2$] = 7.45 $\cdot 10^{-12}$ Pa⁻¹ (at m = 0.115). The 1–3 composite from work [a-15] is to be regarded as a limiting case of the 1–0–3 composite studied in this work (Fig. 1,a) at m_i = 0. Graphs in Fig. 3.a,b show that the increase of max g_h^* and max $[(Q_h^*)^2]$ in the 1-0-3 composite is achieved due to the orientation effect in the 0-3 matrix based on the highly anisotropic ceramic. Finally, a 0-3 Sn₂P₂S₆ SC / epoxy composite [a-16] is of interest for a further comparison. According to Ref.a-16, values of $\max g_h^* \approx (150-155) \text{ mV.m/N}$ and $\max d_h^* \approx 55 \text{ pC/N}$ were experimentally determined for 0-3composite samples. With an increasing in the size of the SC inclusions in this composite both g_h^* and d_h^* increase, so that values of $g_h^* \approx 500\,$ mV m/N and max $d_h^* \approx 150\,$ pC/N are acheived in specific ranges of the sizes of the Sn₂P₂S₆ SC inclusions. The corresponding composite exhibits predominantly the 1–3-type connectivity that leads to an improved hydrostatic piezoelectric response due to a continuous distribution of the piezoelectric Sn₂P₂S₆ inclusions along the poling axis.

Thus, we have observed advantages of the piezoelectric performance of the novel 1–0–3 composite based on the relaxor-ferroelectric SC over the performance of the two-component

ceramic / polymer and SC / polymer composites, and these advantages are achieved due to the strong longitudinal piezoelectric effect and the considerable hydrostatic piezoelectric response.

4. Conclusions

A new *orientation effect* has been first studied in novel three-component 1–0–3 composites (Fig. 1,a) with two contrasting ferroelectric components, namely, the highly piezo-active relaxor-ferroelectric PMN–0.33PT SC (rods) and highly anisotropic (Pb_{1–x}Ca_x)TiO₃ ceramic (inclusions, x=0.20–0.25). The effective electromechanical properties (3) and related parameters (4)–(7) of this composite are functions of four variables, m, m_i , ρ_i , α , and this circumstance makes a problem of optimisation of the properties a difficult task.

Changes in the rotation angle $\alpha = (P_s^{(1)} \wedge P_r^{(2)})$ give rise to changes in the elastic and piezoelectric anisotropy of the 0-3 matrix. The $(Pb_{1-x}Ca_x)TiO_3$ ceramic plays an important role in the orientation effect due to the very large anisotropy of the piezoelectric coefficients $d_{3j}^{(2)}$ in comparison to the anisotropy of $d_{3j}^{(1)}$ of the PMN-0.33PT SC (see Table 1) and due to the high elastic anisotropy. Ceramic inclusions with a prolate shape promote considerable elastic and piezoelectric anisotropy of the 0-3 matrix and an appreciable orientation effect in the 1-0-3 composite. A comparison of the effective parameters (6) and (7) of this composite due to the parameters of the related 1–3 SC / polymer composite enables us to emphasise the high performance of the 1–0–3 PMN–0.33PT SC / (Pb_{1-x}Ca_x)TiO₃ ceramic / araldite composite (x=0.20–0.25). It worth noting that maxima of its three hydrostatic parameters, d_h^* , g_h^* and $(Q_h^*)^2$, are achieved at a volume fraction of the ceramic inclusions m_i = const, and a good correlation between results obtained using the EFM and two versions of the FEM (Table 2) is observed. As follows from Table 2, changes in the mesh of the 0–3 matrix with spheroidal ceramic inclusions does not give rise to significant changes in g_h^* and $(Q_h^*)^2$ which are predicted using the FEM. The orientation effect studied in this 1–0–3 composite leads to a considerable anisotropy of squared figures of merit (8) and electromechanical coupling factors (9) at the relatively high

piezoelectric activity, and such characteristics when combined with large parameters (6) and (7) are of value for hydroacoustic, piezoelectric energy harvesting and transducer applications.

Acknowledgements

The authors would like to thank Prof.Dr. R. Stevens (University of Bath, UK), Prof.Dr. A.E. Panich, Prof.Dr. A.A. Nesterov, Prof. Dr.I.A. Parinov (Southern Federal University, Russia), and Prof.Dr. S.-H. Chang (National Kaohsiung Marine University, Taiwan, ROC) for their research interest in the piezoelectric performance and hydrostatic parameters of advanced composite materials suitable for underwater applications. Prof.Dr. C.R. Bowen acknowledges funding from the European Research Council under the European Union's Seventh Framework Programme (FP/2007-2013) / ERC Grant Agreement no. 320963 on Novel Energy Materials, Engineering Science and Integrated Systems (NEMESIS). The research subject is also concerned with the Programme Supporting the Research at the Southern Federal University (Russia).

References

- [a-1] E.K. Akdogan, M. Allahverdi, A. Safari, IEEE Trans. Ultrason., Ferroelec., Freq. Contr. 52 (2005) 746–775.
- [a-2] A. Safari, E.K. Akdogan, Ferroelectrics 331 (2006) 153–179.
- [a-3] H. Taunaumang, H. Guy, H.L.W. Chan, Journal of Applied Physics 76 (1994) 484–489.
- [a-4] J. Bennett, G. Hayward, IEEE Trans. Ultrason., Ferroelec., Freq. Contr. 44 (1997) 565–574.
- [a-5] F. Wang, C. He, Y. Tang, Mater. Chem. Phys. 105 (2007) 273–277.
- [1] V.Yu. Topolov, C.R. Bowen, P. Bisegna, S.E. Filippov, The piezoelectric performance and anisotropy factors of modern three-component composites, in: I.A. Parinov (Ed.), Nano- and Piezoelectric Technologies, Materials and Devices, Nova Sci. Publ., New York, 2013, pp.51–78.
- [2] V.Yu. Topolov, P. Bisegna, C.R. Bowen, Piezo-active Composites. Orientation Effects and Anisotropy Factors, Springer, Berlin, Heidelberg, 2014.
- [a-6] C.-W. Nan, G.J. Weng, J. Appl. Phys. 88 (2000) 416–423.
- [a-7] K.L. Ng, H.L.W. Chan, C.L. Choy, IEEE Trans. Ultrason., Ferroelec., Freq. Contr. 47 (2000) 1308–1315.
- [a-8] K.H. Lam, H.L.W. Chan, Compos. Sci. Technol. 65 (2005) 1107 –1111.
- [a-8prim] H. Ren, H. Fan, Sensors a. Actuators A 128 (2006) 132–139.
- [a-8duo] C.-W. Nan, L. Liu, D. Guo, L. Li, J. Phys. D: Appl. Phys. 33 (2000) 2977–2984.
- [3] K. Ren, Y. Liu, X. Geng, H.F. Hofmann, Q.M. Zhang, IEEE Trans. Ultrason., Ferroelec., Freq. Contr. 53 (2006) 631–638.
- [4] S.A. Wilson, G.M. Maistros, R.W. Whatmore, J. Phys. D: Appl. Phys. 38 (2005) 175–182.
- [a-9] J.H. Huang, S. Yu, Compos. Engin. 11 (1994) 1169–1182.
- [a-10] COMSOL, Inc. COMSOLMultiphysicsTM User's Guide (version 3.5a, 2008),
- http://www.comsol.com
- [a-11] W. Hacksbusch, Multi-grid Methods and Applications, Springer, Berlin, 1985.
- [a-12] T. Ikeda, Fundamentals of Piezoelectricity, Oxford University Press, Oxford, New York,

Toronto, 1990.

- [a-13] K.H. Yoon, J.H. Yoo, W.S. Kim, E.S. Kim, Ferroelectrics 186 (1996) 169–172.
- [a-14] C.J. Dias, D.K. Das-Gupta, Electroactive polymer-ceramic composites, in: Proceedings of the 4th International Conference on Properties and Applications of Dielectric Materials, July 3–8, 1994, Brisbane, Australia, IEEE, New York, 1994, pp.175–178.
- [5] R. Zhang, B. Jiang, W. Cao, J. Appl. Phys. 90 (2001) 3471–3475.
- [6] S.V. Glushanin, V.Yu. Topolov, A.V. Krivoruchko, Mater. Chem. Phys. 97 (2006) 357–364.
- [7] F. Levassort, M. Lethiecq, C. Millar, L. Pourcelot, IEEE Trans. Ultrason., Ferroelec., Freq. Contr. 45 (1998) 1497–1505.
- [8] Y. Xu, Ferroelectric Materials and Their Applications, North-Holland, Amsterdam, London, New York, Toronto, 1991.
- [a-15] S.V. Bezus, V.Yu. Topolov, C.R. Bowen, J. Phys. D: Appl. Phys. 39 (2006) 1919–1925.[a-16] M.M. Maior, I.P. Prits, Yu.M. Vysochanskii, Ferroelectrics 266 (2002) 247–257.

Table 1. Elastic compliances s_{ab}^{E} (in 10^{-12} Pa⁻¹), piezoelectric coefficients d_{fl} (in pC/N) and relative dielectric permittivities $\varepsilon_{rr}^{\sigma}/\varepsilon_{0}$ of components at room temperature

Component	s_{11}^E	S_{12}^E	S_{13}^E	S_{33}^E	S_{44}^E	S_{66}^E	d_{31}	<i>d</i> ₃₃	d_{15}	$arepsilon_{11}^{\sigma}/arepsilon_0$	$\mathcal{E}_{33}^{\sigma}/\mathcal{E}_{0}$
PMN–0.33PT SC, 4mm symmetry [5]	69.0	-11.1	-55.7	119.6	14.5	15.2	-1330	2820	146	1600	8200
(Pb _{0.80} Ca _{0.20})TiO ₃ ceramic [6]	6.04	-1.24	-1.25	6.21	14.7	14.6	-1.33	24.6	26.1	131	135
(Pb _{0.75} Ca _{0.25})TiO ₃ ceramic [6]	6.00	-1.30	-1.30	6.18	14.8	14.6	-0.364	28.0	28.9	158	163
Araldite [7]	216	-78	-78	216	588	588	0	0	0	4.0	4.0

Table 2. Hydrostatic piezoelectric coefficient g_h^* (in mV·m / N) and squared hydrostatic figure of merit $(Q_h^*)^2$ (in 10^{-12} Pa⁻¹) of the 1–0–3 PMN–0.33PT SC / (Pb_{0.80}Ca_{0.20})TiO₃ ceramic / araldite composite at $\rho_i = 0.1$ and $\alpha = 90^\circ$. Methods for prediction of properties of the 0–3 matrix are listed in the 1st column

Methods	g_h^* at	g_h^* at	g_h^* at	g_h^* at	g_h^* at	g_h^* at	$(Q_h^*)^2$ at	$(Q_h^*)^2$ at	$(Q_h^*)^2$ at
	$m_i=0.10,$	$m_i=0.10,$	$m_i=0.10,$	$m_i=0.15$,	$m_i=0.15$,	$m_i=0.15$,	$m_i=0.10,$	$m_i=0.10,$	$m_i=0.10,$
	m = 0.05	m = 0.06	m = 0.10	m = 0.05	m = 0.06	m = 0.10	m = 0.10	m = 0.12	m = 0.15
EFM	133	121	86.6	133	122	89.1	10.2	10.3	10.0
FEM-1a	139	128	92.2	139	129	95.5	11.1	11.2	11.0
FEM-2 ^b	128	117	84.3	127	118	86.5	9.53	9.59	9.40
Methods	$(Q_h^*)^2$ at	$(Q_h^*)^2$ at	$(Q_h^*)^2$ at						
	$m_i=0.15,$	$m_i=0.15,$	$m_i=0.15,$						
	m = 0.10	m = 0.12	m = 0.15						
EFM	10.3	10.4	10.2						
FEM-1a	11.0	11.2	11.1						
FEM-2 ^b	9.32	9.46	9.36	•					

^aWith a coarse mesh and higher piezoelectric activity of the 0–3 matrix

^bWith a fine mesh and lower piezoelectric activity of the 0–3 matrix

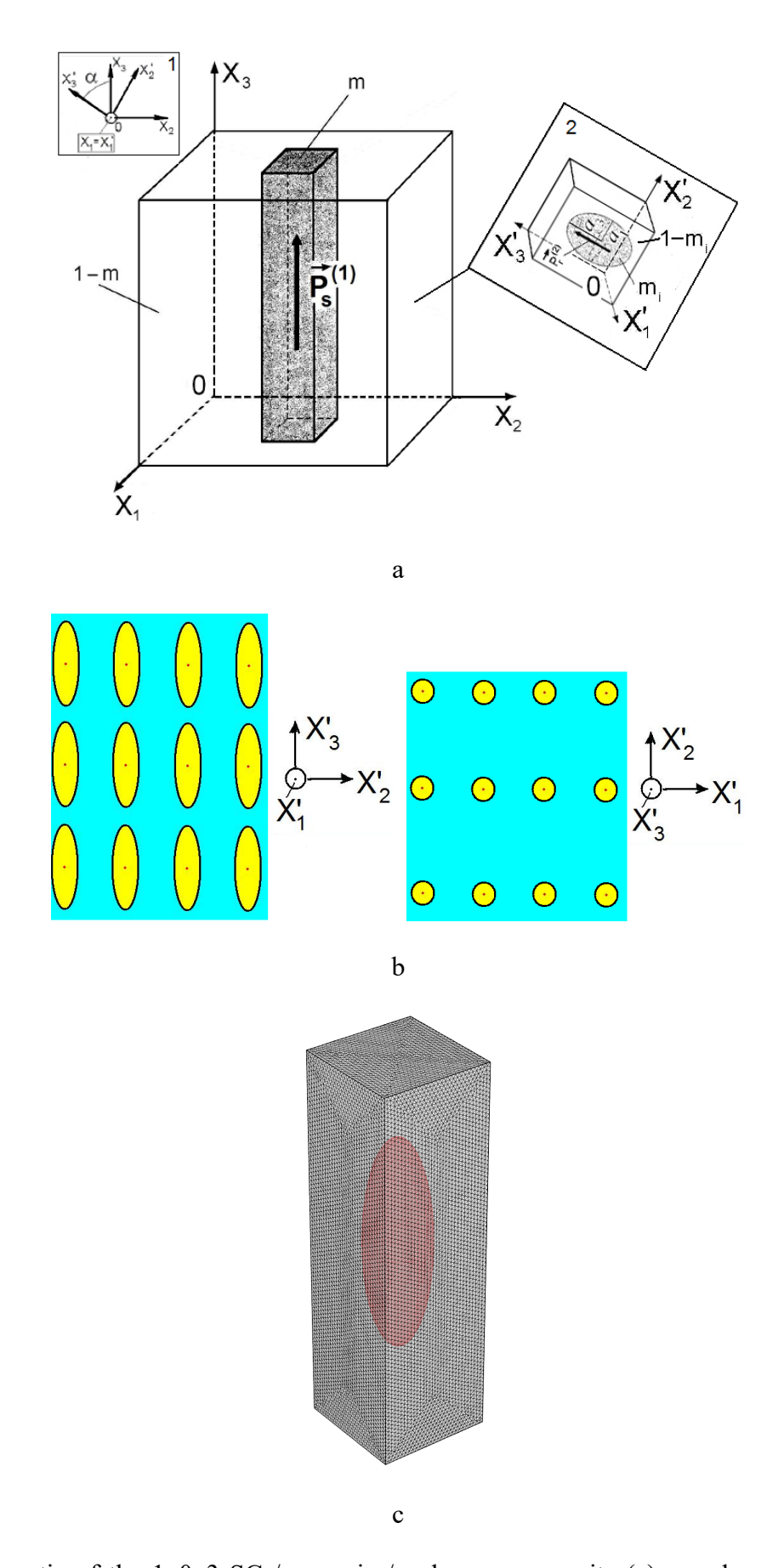


Fig. 1. Schematic of the 1–0–3 SC / ceramic / polymer composite (a), regular arrangement of spheroidal ceramic inclusions in the 0–3 matrix along the co-ordinate axes $OX_{k'}$ (b) and mesh (c)

used in finite element modeling for the 0–3 matrix. m and 1 - m are volume fractions of the SC and surrounding 0–3 matrix, respectively. Rotation of co-ordinate axes $(X_1'X_2'X_3') \rightarrow (X_1X_2X_3)$ is shown in inset 1 of Fig.1,a, the 0–3 matrix is shown in inset 2 of Fig.1,a. In the 0–3 matrix, m_i and $1 - m_i$ are volume fractions of the ceramic and polymer, respectively.

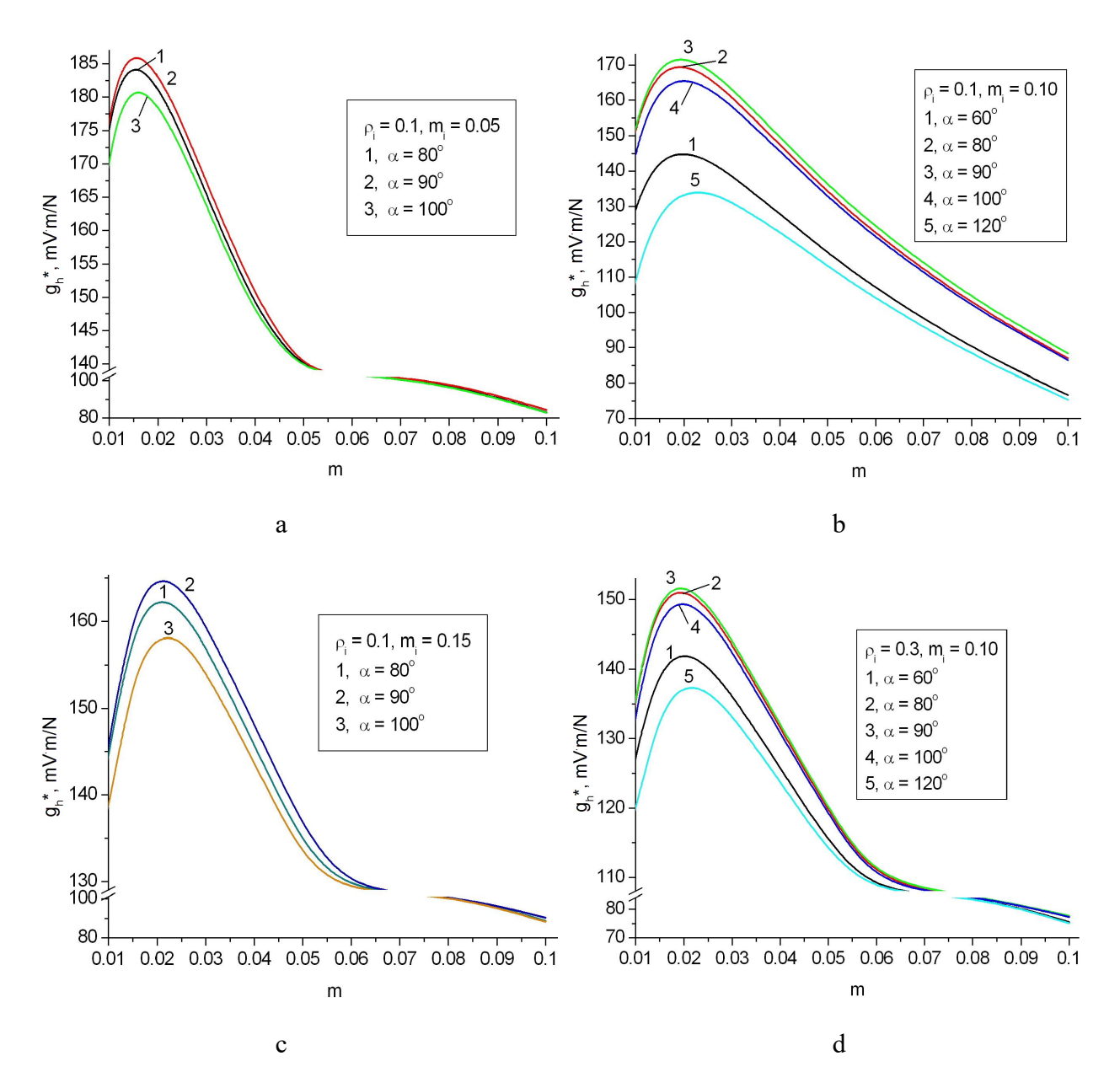


Fig. 2. Examples of local max $g_h^*(m, m_i, \rho_i, \alpha)$ of the 1–0–3 PMN–0.33PT SC / (Pb_{0.75}Ca_{0.25})TiO₃ ceramic / araldite composite at ρ_i = 0.1 (a–c) and ρ_i = 0.3 (d). Values of g_h^* are given in mV·m/N. Electromechanical properties of the 0–3 matrix at the first stage of averaging were determined by means of the EFM.

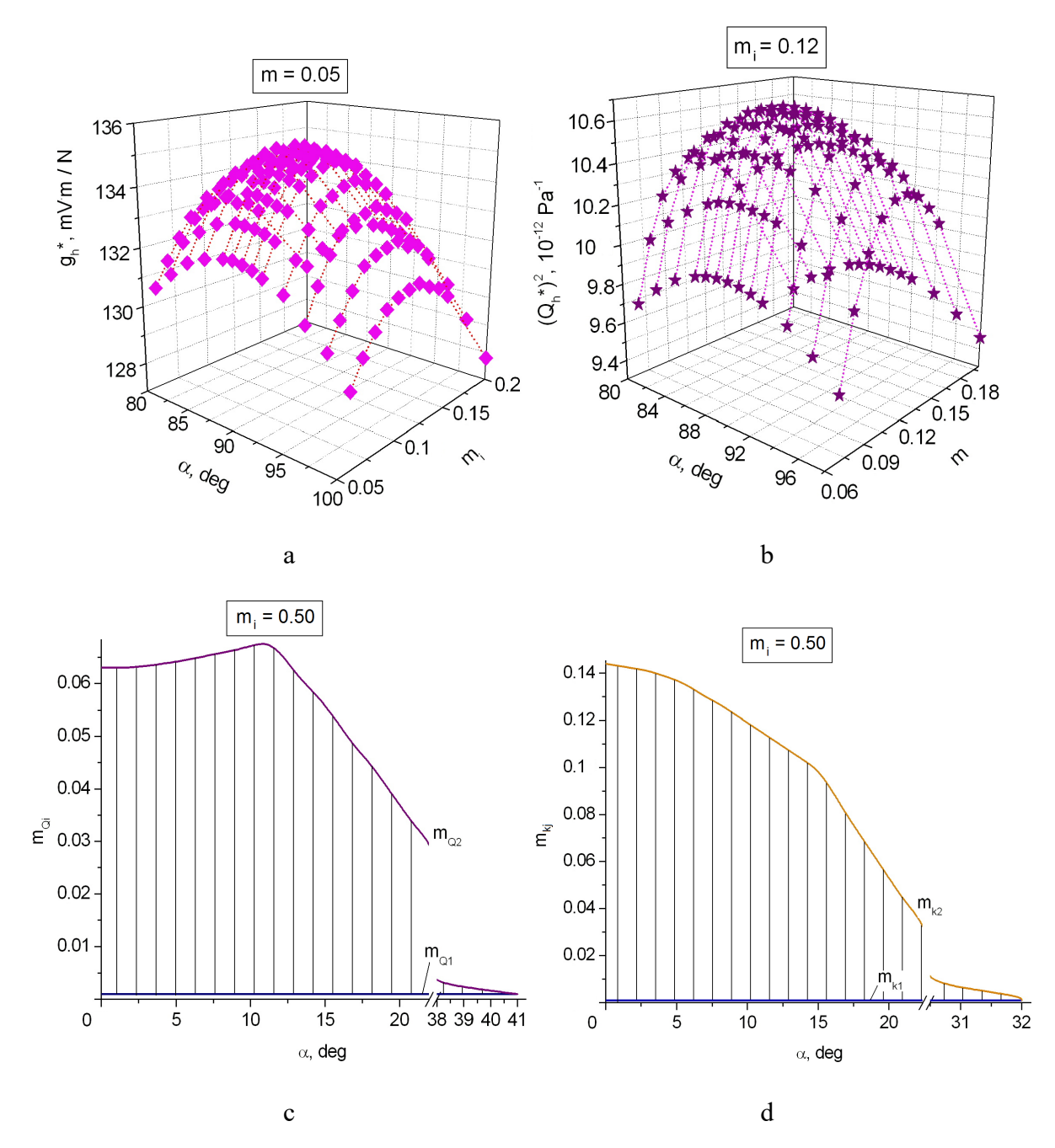


Fig. 3. Examples of the high piezoelectric performance of the 1–0–3 PMN–0.33PT SC / (Pb_{0.75}Ca_{0.25})TiO₃ ceramic / araldite composite at ρ_i = 0.1: (a) near local max g_h^* (0.05, m_i , 0.1, α), (b) near absolute max {[Q_h^* (m, 0.12, 0.1, α)]²}, (c) region of validity of condition (8) (hatched area) at m_i = 0.50, (d) region of validity of condition (9) (hatched area) at m_i = 0.50, (e) and (f) d_{3j}^* (0.05, m_i , 0.1, α) and g_{3j}^* (0.05, m_i , 0.1, α) near local extreme points. Electromechanical properties of the 0–3 matrix at the first stage of averaging were determined by means of the EFM.

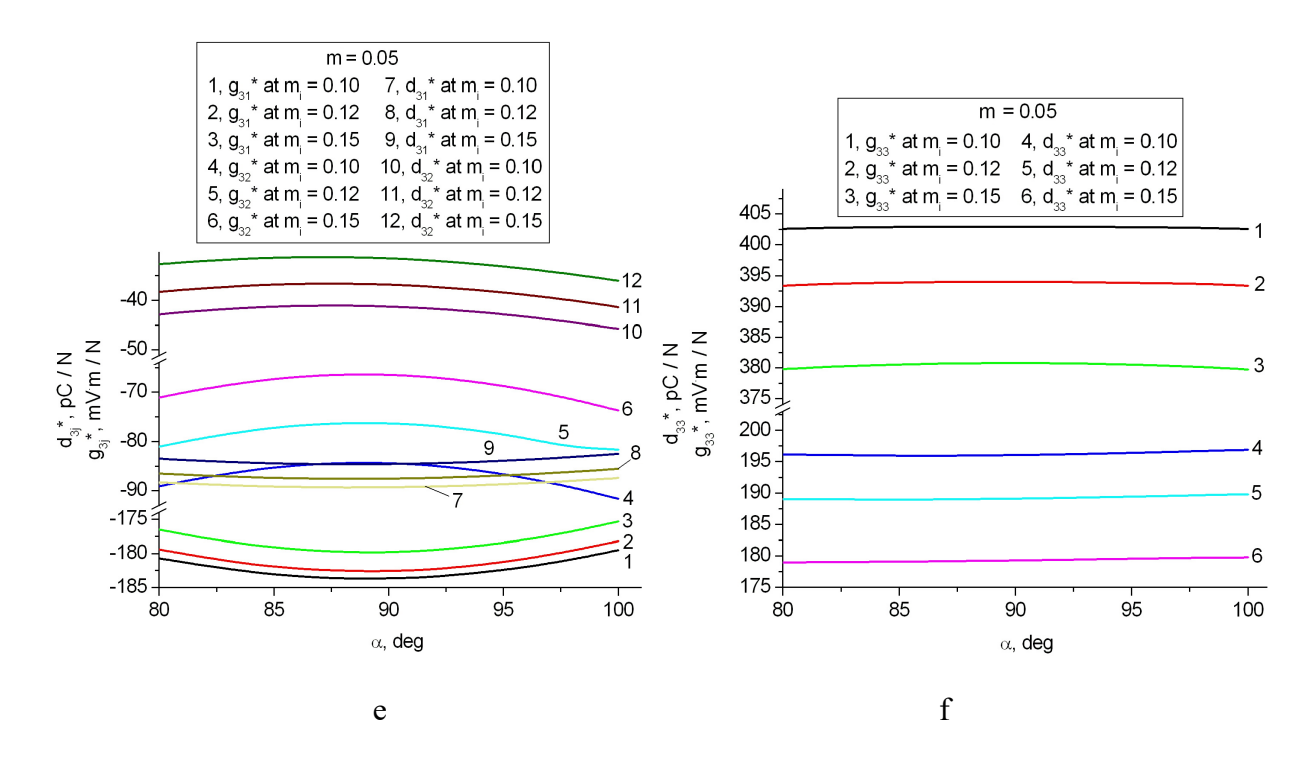


Fig. 3 (continued)